

Real-Time Privacy Preservation for Robot Visual Perception

Minkyu Choi*, Yunhao Yang*, Neel P. Bhatt*, Kushagra Gupta, Sahil Shah, Aditya Rai,
David Fridovich-Keil, Ufuk Topcu, Sandeep P. Chinchali
The University of Texas at Austin
Austin, Texas, USA

Abstract—Many robots (e.g., iRobot’s Roomba) operate based on visual observations from live video streams, and such observations may inadvertently include privacy-sensitive objects, such as personal identifiers. Existing approaches for preserving privacy rely on deep learning models, differential privacy, or cryptography. They lack guarantees for the complete concealment of all sensitive objects. Guaranteeing concealment requires post-processing techniques and thus is inadequate for real-time video streams. We develop a method for privacy-constrained video streaming, PCVS, that conceals sensitive objects within real-time video streams. PCVS takes a logical specification constraining the existence of privacy-sensitive objects, e.g., never show faces when a person exists. It uses a detection model to evaluate the existence of these objects in each incoming frame. Then, it blurs out a subset of objects such that the existence of the remaining objects satisfies the specification. We then propose a conformal prediction approach to (i) establish a theoretical lower bound on the probability of the existence of these objects in a sequence of frames satisfying the specification and (ii) update the bound with the arrival of each subsequent frame. Quantitative evaluations show that PCVS achieves over 95 percent specification satisfaction rate in multiple datasets, significantly outperforming other methods. The satisfaction rate is consistently above the theoretical bounds across all datasets, indicating that the established bounds hold. Additionally, we deploy PCVS on robots in real-time operation and show that the robots operate normally without being compromised when PCVS conceals objects.

I. INTRODUCTION

While robots utilize visual observations from video streams during operational routines for decision-making purposes, recording and disseminating such videos potentially exposes private information [12], raising ethical and legal concerns. These concerns include risks of the inadvertent capture of sensitive personal data, unauthorized access, and misuse of recorded footage. A recent story highlighting a Roomba taking images of a person in a toilet room attests to the legitimacy of privacy concerns during robotic operations [10].

Existing approaches protect privacy by concealing sensitive objects, but they either fail to guarantee complete concealment or cannot process real-time video streams. While concealing sensitive objects requires detecting and locating such objects, existing works rely on deep-learning models for object detection [18, 24, 11]. However, due to their black-box nature, deep-learning models cannot provide theoretical guarantees on the correctness of the detection results. On the other hand, formal methods techniques, such as model checking, can guarantee

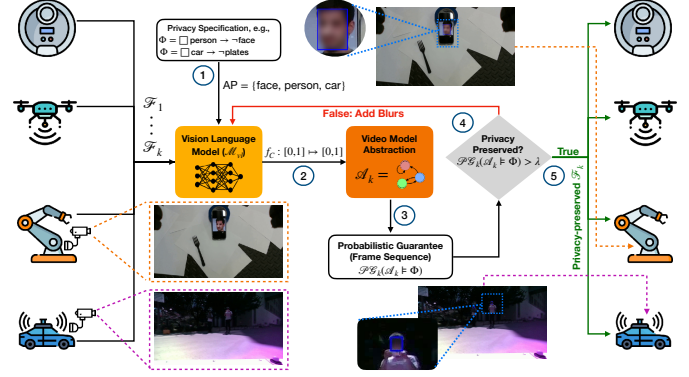


Figure 1: **Pipeline of Privacy-Constrained Video Streaming:** (Step 1) Given a privacy specification Φ , we define a set AP of atomic propositions describing privacy-sensitive objects. (Step 2) Given an incoming frame \mathcal{F}_k from the video, the method uses a vision-language model (VLM) to detect sensitive objects in the frame. Each detection is associated with a confidence score from the VLM. The method calibrates a confidence score to a per-frame probability bound for correct detection via a calibration function f_C , as in Equation 1. (Step 3) The method builds an abstract model \mathcal{A}_k representing object detections and their probability bounds in the frame sequence $\mathcal{F}_1, \dots, \mathcal{F}_k$ via Algorithm 1. Then, it computes a theoretical bound for the probability of \mathcal{A}_k satisfying Φ , i.e., a probabilistic guarantee $\mathcal{PG}_k(\mathcal{A}_k \models \Phi)$ using Equation 3. (Step 4) If $\mathcal{PG}_k(\mathcal{A}_k \models \Phi)$ is below a user-given privacy threshold λ , the method removes a subset of sensitive objects and goes back to Step 2 to recompute a guarantee. (Step 5) If $\mathcal{PG}_k(\mathcal{A}_k \models \Phi)$ is above λ , the method adds \mathcal{F}_k back to the stream and proceeds to Step 1 with the next incoming frame. We number each step in blue.

that a given video adheres to privacy concerns [25, 31, 7]. However, the computational complexity of formal methods techniques grows with the video length, hence incapable of real-time video streams.

We develop a method to conceal privacy-sensitive objects in real-time video streams from robot cameras. The method takes a logical specification constraining the existence of sensitive objects. The specifications allow users to describe complex privacy requirements with conjunctions, disjunctions, implications, etc. For each incoming frame from the video

*These authors contributed equally to this work.

streams, the method first uses a vision-language model to detect and locate all sensitive objects. Next, it removes a subset of objects (add Gaussian blurs or blackout) so that the existence of the remaining objects satisfies the specification.

We then establish a theoretical bound on the probability of complete concealment of sensitive objects in a video stream. As deep learning models are typically over-confident in detecting objects, we use conformal prediction to calibrate the model’s confidence to a probability of correct detection. Next, we express the specification as a temporal logic formula and build a finite automaton representing the object detections in a sequence of frames and the probabilities of correct detections. Then, we compute the probability that this automaton satisfies the specification (i.e., the video frames encountered so far preserve privacy).

We develop a video abstraction algorithm that allows us to optimize the computational complexity involved with the arrival of each subsequent frame from the video stream. This abstraction is key to our method achieving real-time performance, updating the probability with each frame arrival. This probability acts as a metric and helps users determine whether to use the video based on their privacy tolerance.

We evaluate the method over two large-scale datasets and present real-robot examples for real-time privacy protection. The method achieves 80 to 97 percent specification satisfaction rates in various scenarios, significantly outperforming existing automated solutions. Meanwhile, the method preserves all non-sensitive information. By seamlessly integrating concealment capabilities into the robot’s visual perception system, we prevent potential privacy leakage from the robot. Simultaneously, this integration ensures the unhindered functionality of the robot’s control policies, enabling it to operate normally without compromise.

II. RELATED WORK

Privacy preservation in real-time video analytics has been the focus of several recent methods [18, 24, 11, 8, 29, 28, 16, 33, 26]. However, they rely solely on deep learning models for object detection, i.e., detecting and blurring privacy-sensitive entities in video. Due to the black-box nature of neural networks, these methods lack a quantitative guarantee.

To this end, formal verification approaches have guaranteed that a given complete video adheres to privacy safety concerns formulated as temporal logical specifications. For example, recent works [25, 31, 7, 6, 23, 32] construct a finite automaton representing video frame sequences and verify this automaton against temporal logical specifications. However, their approaches do not account for uncertainties related to the vision-based detection algorithms [3]. Moreover, the construction and verification of automata cannot be done in real-time.

On the other hand, some works using differential privacy or cryptography do not rely on deep learning models and, hence, can provide theoretical guarantees. For instance, Cangialosi et al. [4] developed a differential privacy mechanism to protect video privacy, and Rahman et al. [19] propose a cryptographic approach for video privacy. However, without integrating

with deep learning models, these methods cannot interpret and enforce complex privacy requirements. In contrast, our method enforces the video satisfying any complex privacy requirements expressed in logic formulas.

III. PROBLEM FORMULATION

A video \mathcal{V} is a sequence of frames $\mathcal{F}_1, \dots, \mathcal{F}_k$ where each $\mathcal{F}_k \in \mathbb{R}^{C \times W \times H}$ is an RGB image with C channels, W width, and H height. A video can be prerecorded or live-streamed from sources such as autonomous vehicles or security cameras.

We define a **privacy specification** Φ as a temporal logic formula [21] constraining the appearance of privacy-sensitive objects. Since we want to preserve privacy at all times, we express a privacy specification as $\Phi = \Box(\tilde{\Phi})$, where \Box represents the “ALWAYS” temporal operation and $\tilde{\Phi}$ is a first-order logic formula [2]. The presence of privacy-sensitive objects is constrained by Φ .

We define a set of atomic propositions AP , where each proposition $p_i \in AP$ is a textual description of a privacy-sensitive object. Then, we use a vision-language model (VLM), \mathcal{M}_{vl} , to detect these objects. $\mathcal{M}_{vl} : \mathbb{R}^{C \times W \times H} \times AP \rightarrow [0, 1]$ takes a frame $\mathcal{F}_k \in \mathbb{R}^{C \times W \times H}$ and a proposition $p_i \in AP$ as inputs, and returns a confidence score $c \in [0, 1]$, denoted as $c = \mathcal{M}_{vl}(\mathcal{F}_k, p_i)$. However, deep learning models are often overconfident, and their detection accuracy cannot be guaranteed. Therefore, we calibrate the confidence using conformal prediction [22], which provides a lower bound for the probability of correctly detecting privacy-sensitive objects in every frame, considering the inherent uncertainty in deep learning model predictions.

However, traditional conformal prediction approaches focus on post-processing and do not account for temporal events. Therefore, we use calibrated confidence to detect and constrain privacy-sensitive objects over time and provide a probabilistic guarantee on a sequence of frames.

To achieve this, we develop an algorithm \mathcal{VA} that takes a sequence of k frames and returns a formally verifiable video abstraction \mathcal{A}_k encoding the object detection across the sequence: $\mathcal{VA}([\mathcal{F}_1, \dots, \mathcal{F}_k]) = \mathcal{A}_k$. The **video abstraction** \mathcal{A}_k is represented as a labeled Markov chain, detailed rigorously in Section IV as it requires extensive background and mathematical notation. This provides a probabilistic guarantee on a frame sequence via formal verification [30].

Definition 1 (Probabilistic Guarantee on a Frame Sequence). Given a sequence of frames $\mathcal{F}_1, \dots, \mathcal{F}_k$, a privacy specification Φ , and a video abstraction \mathcal{A}_k at the k^{th} frame, a probabilistic guarantee $\mathcal{PG}_k(\mathcal{A}_k \models \Phi)$ on the frame sequence $\mathcal{F}_1, \dots, \mathcal{F}_k$ represents the theoretical minimum probability that the presence of privacy-sensitive objects in the frame \mathcal{F}_1 through \mathcal{F}_k adheres to Φ .

Problem 1 (Real-Time Video Privacy Preservation). Given a frame sequence $\mathcal{F}_1, \dots, \mathcal{F}_{k-1}$, an incoming frame \mathcal{F}_k from a video stream, a privacy specification Φ , and an algorithm \mathcal{VA} that builds a video abstraction from the frame sequence, we aim to remove privacy-sensitive objects in \mathcal{F}_k

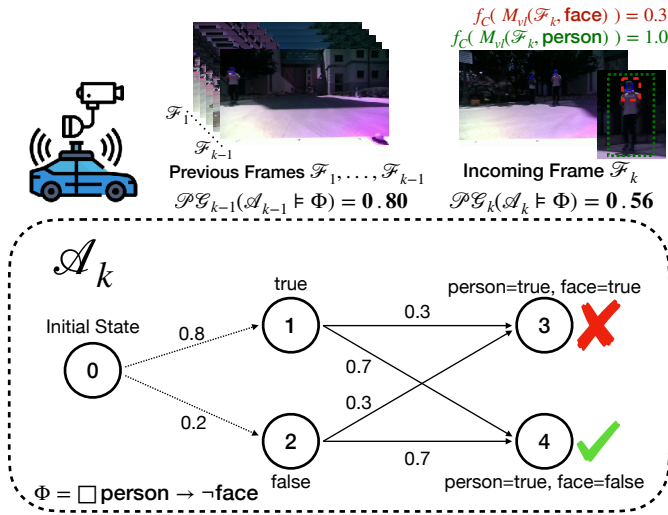


Figure 2: A running example on how to compute the probabilistic guarantee via video abstraction.

such that $\mathcal{A}_k = \mathcal{VA}([\mathcal{F}_1, \dots, \mathcal{F}_k])$ satisfies Φ with a probability at least $\mathcal{PG}_k(\mathcal{A}_k \models \Phi)$.

IV. PRIVACY-CONSTRAINED VIDEO STREAMING

We develop privacy-constrained video streaming (PCVS), a method to enforce live video streams that satisfy a user-given privacy specification with a probabilistic guarantee. The overall pipeline for PCVS is illustrated in Figure 1.

a) Real-Time Video Privacy Preservation Framework:

We explain our framework with a running example in a real-time video stream from a real robot (see Figure 2). We aim to hide human faces so that no personal identity will be revealed in vision-based robot operations. Therefore, the privacy specification is $\Phi = \Box \text{person} \rightarrow \neg \text{face}$, where \rightarrow and \neg mean “implies” and “not,” respectively. We detect humans and faces at every frame via the VLM. Subsequently, we use conformal prediction to obtain a calibrated confidence score for the detection in the current frame. We build a video abstraction \mathcal{A}_k to represent the detection results for humans and faces across a sequence of frames and utilize it to obtain a probabilistic guarantee on Φ being satisfied. We then verify if the guarantee is above the user-given privacy threshold $\lambda \in [0, 1]$. If this threshold is not met, we iteratively remove the detected faces and update the guarantee $\mathcal{PG}_k(\mathcal{A}_k \models \Phi)$ until the threshold is met.

A. Probabilistic Guarantee on Video Privacy

Given a sequence of k frames and a privacy specification Φ , we compute a probabilistic guarantee $\mathcal{PG}_k(\mathcal{A}_k \models \Phi)$. This guarantee is updated at each incoming frame. We use formal methods to prove that the guarantee holds.

a) Confidence Calibration via Conformal Prediction:

Recall that a VLM $\mathcal{M}_{vl}(x_i, y_i) = c$ receives an image x_i and a textual object label y_i as a prompt and returns a confidence score $c \in [0, 1]$. Given the VLM \mathcal{M}_{vl} and a labeled calibration dataset that is distributed identically to the task domain, using

conformal prediction [22], we learn a calibration function $f_C : [0, 1] \mapsto [0, 1]$ that maps a confidence score, $c \in [0, 1]$ to a lower bound for the probability of correct detection.

We first collect a calibration set $\{(x_i, y_i)\}_{i=1}^m$ consisting of m (image, ground truth text label) tuples. Then, we apply \mathcal{M}_{vl} to detect the privacy-sensitive objects in the images $\{x_i\}_{i=1}^m$ and get a set of *nonconformity scores*: $\{1 - \mathcal{M}_{vl}(x_i, y_i)\}_{i=1}^m$. A nonconformity score is the sum of confidence scores of wrong detections. Next, we estimate a probability density function of these scores, denoted as $f_{nc}(z)$, where z is a nonconformity score. Then, we use Theorem 1 to establish a theoretical lower bound for the probability of the correct detection.

Theorem 1. Let $\epsilon \in [0, 1]$ be a pre-defined error bound and x_n be an image outside the calibration set. We define a *prediction band* as $\hat{C}(x_n) = \{p_i : \mathcal{M}_{vl}(x_n, p_i) \geq 1 - c^*, p_i \in AP\}$. Then, according to conformal prediction, there exists a confidence c^* such that $\epsilon = 1 - \int_0^{c^*} f_{nc}(z) dz$ satisfies $\mathbb{P}[y_n \in \hat{C}(x_n)] \geq 1 - \epsilon$, where y_n is the ground truth label for x_n . Proof in [22].

Note that $\mathcal{M}_{vl}(x_i, p_i)$ returns a single confidence score indicating whether p_i exists in x_i . By the theory of conformal prediction, $1 - \epsilon$ is a theoretical lower bound for the probability of the ground truth label belonging to the prediction band $\hat{C}(x_n)$. If $\mathcal{M}_{vl}(x_i, p_i) > 0.5$, we provide a lower bound for the probability of the existence of p_i . Otherwise, if $\mathcal{M}_{vl}(x_i, p_i) \leq 0.5$, we bound the probability of non-existence. Hence, we get a calibration function

$$f_C(c) = \begin{cases} \int_0^c f_{nc}(z) dz, & \text{if } c > 0.5 \\ \int_0^{1-c} f_{nc}(z) dz, & \text{otherwise.} \end{cases} \quad (1)$$

b) *Video Abstraction.*: For verifying a *real-time* video stream against the privacy specification Φ , a key challenge is to verify the temporal behaviors of *all* the previously received frames plus the current frame. This makes verification space- and time-inefficient because we must repeatedly verify previous frames for each new incoming frame. To overcome this challenge, we build an abstraction for the video stream, which enables real-time verification.

Definition 2 (Video Abstraction). A video abstraction is a labeled Markov chain (S, s_0, P, L) , where S is a set of states, each state corresponds to a conjunction of atomic propositions, $s_0 \in S$ is the initial state, $P : S \times S \rightarrow [0, 1]$ is a transition function. $P(s, s')$ represents the probability of transition from a state s to a state s' and $\sum_{s' \in S} P(s, s') = 1$. $L : S \rightarrow 2^{AP}$ is a labelling function.

We propose Algorithm 1 to build video abstractions. We demonstrate it through an example in Figure 2. First, we add an initial state (State 0 in Figure 2), a state representing the event that all previous frames (if they exist) satisfy Φ (State 1), and a state representing the event that previous frames fail Φ (State 2), as in lines 1-3. Next, we add transitions from State 0 to State 1 and to State 2 with the probability of previous frames satisfying Φ as in line 4. Then, we detect objects

Algorithm 1: Real-Time Video Abstraction

Require: vision-language model \mathcal{M}_{vl} , calibration function f_C , propositions set AP , specification Φ , probability p_{k-1} of previous frames satisfying Φ , incoming frame \mathcal{F}_k

- 1: $S_{\text{obs}}, P, L = \{\}, \{\}, \{\}$ \triangleright Initialize the abstraction
- 2: $S_{\text{obs}}.\text{add}(0), S_{\text{obs}}.\text{add}(1), S_{\text{obs}}.\text{add}(2)$ \triangleright We represent each state with an Arabic numeral
- 3: $L(1) = \text{false}, L(2) = \text{true}$
- 4: $P(0, 1) = 1 - p_{k-1}, P(0, 2) = p_{k-1}$ \triangleright Add transitions to indicate the probability of previous frames satisfying Φ
- 5: $i = 3$ \triangleright Initialize an indexer representing states
- 6: **for** σ in 2^{AP} **do** $\triangleright \sigma$ is a conjunction of atomic propositions
- 7: $\text{prob} = \prod_{p \in \sigma} f_C(\mathcal{M}_{vl}(\mathcal{F}_k, p))$ \triangleright Get a lower bound for a detection result
- 8: **if** $\text{prob} > 0$ **then** \triangleright Add a state to represent the detection with the lower bound
- 9: $S_{\text{obs}}.\text{add}(i), L(i) = \sigma, P(1, i) = \text{prob}, P(2, i) = \text{prob}, i = i + 1$
- 10: **end if**
- 11: **end for**

return $S_{\text{obs}}, s_0 = 0, P, L$

in the incoming frame \mathcal{F}_k and get the probability bound for correct detection. For each conjunction of propositions (e.g., person=true and face=false), we build a state and add transitions to this state with the probability bound of correctly detecting objects described in this conjunction, as in lines 6-9. Hence, we obtain the video abstraction \mathcal{A}_k (e.g., Figure 2).

Following Algorithm 1, we incrementally add new states to the abstraction (rather than build a new one) with the arrival of each new incoming frame and check it against Φ . Hence, this abstraction can be used to check video streams efficiently. Then, we theoretically prove that the probabilistic guarantee obtained through this abstraction holds.

c) Probabilistic Guarantees for Frame Sequence: Given a video abstraction $\mathcal{A} = (S, s_0, P, L)$, we define a *path* π as a sequence of states starting from s_0 . The states evolve according to the transition function P . A *prefix* is a finite path fragment starting from s_0 . We define a *trace* as $\psi = \text{trace}(\pi) = L(s_0)L(s_1)L(s_2)\dots$, where $s_0, s_1, s_2, \dots \in \pi$. $\text{Traces}(\mathcal{A})$ denotes the set of all traces from \mathcal{A} . Each trace $\psi = L(s_0)L(s_1)L(s_2)\dots$ is associated with a probability $\mathbb{P}(\psi) = P(s_0, s_1) \times P(s_1, s_2) \times \dots$

The privacy specification is in the form of $\Box \tilde{\Phi}$. Hence, a privacy specification describes a *safety property* [1].

Definition 3 (Safety Property). A safety property P_{safe} is a set of traces in $(2^{AP})^\omega$ (ω indicates infinite repetitions) such that for all traces $\psi \in (2^{AP})^\omega \setminus P_{\text{safe}}$, there exists a finite prefix $\hat{\psi}$ of ψ such that $P_{\text{safe}} \cap \{\psi' \in (2^{AP})^\omega \mid \hat{\psi} \text{ is a prefix of } \psi'\} = \emptyset$. $\hat{\psi}$ is a *bad prefix* and $\text{BadPref}(P_{\text{safe}})$ is the set of all bad prefixes with respect to P_{safe} .

A video satisfies the privacy specification if its abstract

representation \mathcal{A} satisfies the safety property P_{safe} , i.e., $\text{Traces}(\mathcal{A}) \subseteq P_{\text{safe}}$. The probability that a video satisfies the specification is

$$\begin{aligned} \mathbb{P}[\mathcal{A} \text{ is safe}] &= \mathbb{P}[\pi \in \text{path}(s_0) \mid \text{trace}(\pi) \in P_{\text{safe}}] \\ &= \sum_{\psi \in \text{Traces}(\mathcal{A}) \cap P_{\text{safe}}} \mathbb{P}(\psi). \end{aligned} \quad (2)$$

Note that this probability is a probabilistic guarantee on a sequence of frames. According to the definition of safety property, we derive the following theorem:

Theorem 2. Consider a set of prefixes $\hat{\Psi}$ such that $\mathbb{P}\{\hat{\psi} \in \hat{\Psi} \mid \hat{\psi} \notin \text{BadPref}(P_{\text{safe}})\} \geq \alpha$. Let $\bar{S} \subset S$ be a subset of states in \mathcal{A} such that $\mathbb{P}\{\hat{\psi}L(s) \notin \text{BadPref}(P_{\text{safe}}) \mid \hat{\psi} \notin \text{BadPref}(P_{\text{safe}}) \text{ and } s \in \bar{S}\} \geq \beta$. Then, $\mathbb{P}\{\hat{\psi}L(s) \notin \text{BadPref}(P_{\text{safe}}) \mid s \in \bar{S} \text{ and } \hat{\psi} \in \hat{\Psi}\} \geq \alpha\beta$.

Proof: Let $A = \{\hat{\psi}L(s) \notin \text{BadPref}(P_{\text{safe}}) \mid s \in \bar{S} \cap \hat{\psi} \in \hat{\Psi}\}$ and $B = \{\hat{\psi} \notin \text{BadPref}(P_{\text{safe}}) \mid \hat{\psi} \in \hat{\Psi}\}$. Then, $A|B = \{\hat{\psi}L(s) \notin \text{BadPref}(P_{\text{safe}}) \mid s \in \bar{S} \cap \hat{\psi}L(s) \notin \text{BadPref}(P_{\text{safe}})\}$ and $\mathbb{P}(A) = \mathbb{P}(A|B) \cdot \mathbb{P}(B) \geq \alpha\beta$. ■

From Theorem 2, we can compute a new probabilistic guarantee on a sequence of frames after each incoming frame. However, the length of the abstraction's prefixes increases as the stream continues, leading to high complexity. Therefore, we derive the following proposition to show that Theorem 2 holds even if we fix the length of the prefixes (proof of the proposition is in the Appendix):

Proposition 1. Let $\hat{\psi}_T$ and $\hat{\psi}_F$ be single element prefixes whose corresponding paths only consist of one state such that $\hat{\psi}_T \notin \text{BadPref}(P_{\text{safe}})$ and $\hat{\psi}_F \in \text{BadPref}(P_{\text{safe}})$. Let $\mathbb{P}(\hat{\psi}_T) = \alpha, \mathbb{P}(\hat{\psi}_F) = 1 - \alpha, \Psi' = \{\psi_T, \psi_F\}$, then if we replace $\hat{\Psi}$ with Ψ' in Theorem 2, the Theorem still holds.

Proof: Since $\mathbb{P}(\hat{\psi}_T) = \alpha$ and $\mathbb{P}(\hat{\psi}_F) = 1 - \alpha$, $\mathbb{P}\{\hat{\psi} \in \Psi' \mid \hat{\psi} \notin \text{BadPref}(P_{\text{safe}})\} = \alpha$. The replacement of $\hat{\Psi}$ with Ψ' does not affect $\mathbb{P}\{\hat{\psi}L(s) \notin \text{BadPref}(P_{\text{safe}}) \mid \hat{\psi} \notin \text{BadPref}(P_{\text{safe}}) \cap s \in \bar{S}\}$. Thus, the conditions of Theorem 2 are satisfied, and $\mathbb{P}\{\hat{\psi}L(s) \notin \text{BadPref}(P_{\text{safe}}) \mid s \in \bar{S} \cap \hat{\psi} \in \Psi'\} \geq \alpha\beta$. ■

From Theorem 2 and Proposition 1, we can compute $\mathcal{PG}_k(\mathcal{A}_k \models \Phi)$ as follows:

$$\begin{aligned} \mathcal{PG}_k(\mathcal{A}_k \models \Phi) &= \mathcal{PG}_{k-1}(\mathcal{A}_{k-1} \models \Phi) \\ &\quad \times \left(\sum_{\sigma \models \tilde{\Phi}} \prod_{p \in \sigma} f_C(\mathcal{M}_{vl}(\mathcal{F}_k, p)) \right) \end{aligned} \quad (3)$$

The video abstraction captures all previous frames in only two states (States 1 and 2 in Figure 2) instead of accumulating states for every frame in the sequence. Thus, we can efficiently update the guarantee through a single computation. In Figure 2, $\mathcal{PG}_k(\mathcal{A}_k \models \Phi) = 0.8 \times 0.7 = \mathbf{0.56}$.

V. ROBOT DEMONSTRATIONS

Our experiments assess our method in two areas: (i) its ability to protect privacy, and (ii) its efficiency in preserving other features for vision-based robot tasks.



Figure 3: We present the demonstrations for indoor robot navigation (top left), ground robot navigation (top right), and urban drone monitoring (bottom left). The indoor robot and the ground robot are shown in the bottom right. Scenes with an ‘x’ in a red circle contain privacy-sensitive objects and our method successfully conceals them. All demonstrations effectively maintain privacy above the user-given privacy threshold of 0.80, denoted as $\mathcal{P}\mathcal{G}_k(\Phi) > 0.80$.

We demonstrate our approach on a Jackal ground robot for autonomous driving, an indoor robot for in-house navigation and service, and a drone for urban monitoring (see Figure 3). Given video streams from robot cameras, we aim to execute actions based on the control policy (π). Our approach effectively preserves privacy with formal guarantees without compromising performance in the real-time robot operation. We use YOLOv9 [27] in our method for all demonstrations.

a) Indoor Navigation: In the first demonstration, we deploy PCVS to an indoor navigation robot to protect user privacy. We ground the robot in a private residence for in-house services such as transporting objects and house cleaning. While the robot perceives the environment through visual observations, we aim to preserve the privacy within such observations. The privacy specification is

$$\Phi_1 = \square (\neg \text{laptop} \wedge \neg \text{medication} \wedge \neg \text{person}),$$

which requires hiding all people, laptops, and medications appearing in the scenes.

Figure 3 (top left) demonstrates how our method performs to conceal the sensitive objects such that the video satisfies the privacy specification. The probabilistic guarantee of privacy preservation throughout the complete operation is 0.81.

b) Ground Robot Driving: We deploy the control policy on the ground robot for five driving tasks, such as turning right at a stop sign (as presented in Figure 4). We embed PCVS in the robot’s camera to conceal sensitive objects during real-time

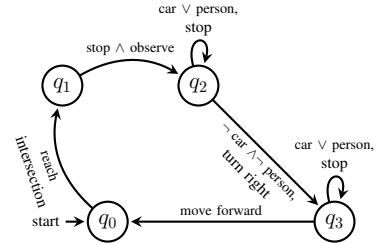


Figure 4: A sample control policy for the ground robot. Each transition is associated with an (input, output) tuple.

operation. In the driving example, we define a set of privacy specifications:

$$\Phi_2 = \square \neg \text{road sign},$$

$$\Phi_3 = \square ((\text{bicycle} \rightarrow \neg \text{person}) \vee (\text{person} \rightarrow \neg \text{face})),$$

$$\Phi_4 = \square ((\text{bus} \vee \text{car}) \rightarrow \neg \text{plate}).$$

Intuitively, we want to conceal privacy-sensitive objects such as road name signs, car plates, and human faces. Figure 3 (top right) presents an example of how our method conceals sensitive objects to satisfy the specifications. The driving operation has a probabilistic guarantee of privacy preservation at 0.84, i.e., at least 84 percent of satisfying the specifications.

When concealing sensitive objects, it is crucial to ensure that such concealment does not adversely impact the robot’s decision-making processes. For instance, the robot should still be capable of detecting and avoiding pedestrians even after

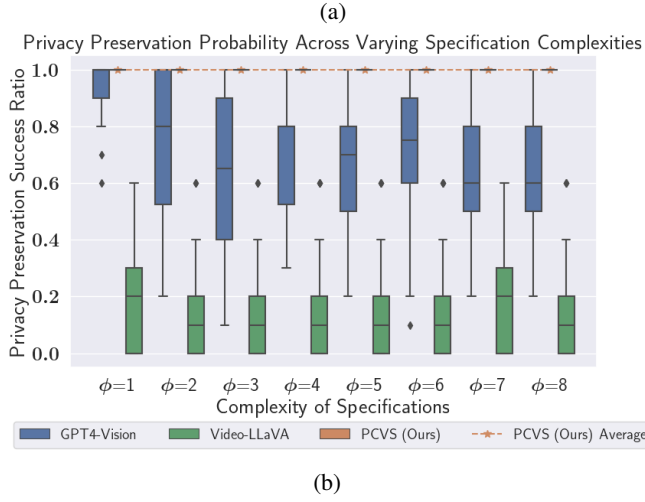
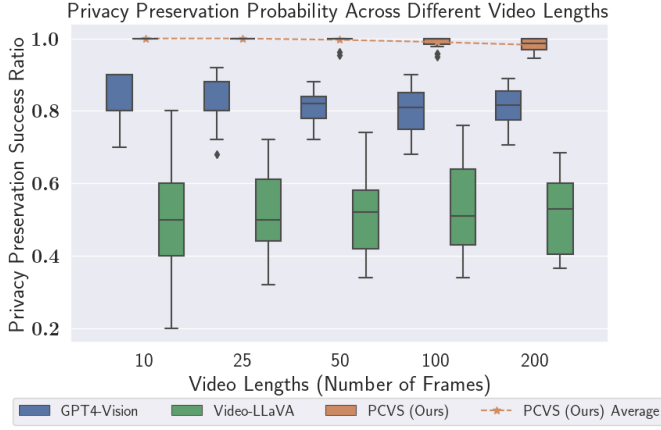


Figure 5: **PCVS effectively maintains privacy in long-horizon videos and complex privacy specifications.** In Figure 5a, PCVS consistently preserves privacy, achieving an average Privacy Preservation Success Ratio of 0.97 across various video lengths. In Figure 5b, we show that PCVS consistently upholds privacy regardless of the complexity of specifications with an average Privacy Preservation Success Ratio of 0.94.

their faces have been obscured. More precisely, consider a safety specification:

$$\Phi_5 = \Box ((\text{car} \vee \text{person}) \rightarrow \mathbf{X} \text{ stop},$$

which necessitates that the robot comes to a stop if cars or pedestrians are present ahead.

In the demonstration, the robot performs identically regardless of whether our method is deployed, and in both cases, it satisfies the safety specifications. Hence, we show that our privacy protection will not over-conceal non-sensitive objects and negatively impact the decision-making procedure in driving scenarios.

c) *Urban Drone Monitoring*: We demonstrate the applicability and effectiveness of our method in urban drone monitoring scenarios. The privacy specification is:

$$\Phi_6 = \Box ((\text{bicycle} \rightarrow \neg \text{person}) \wedge (\text{car} \vee \text{bus} \rightarrow \neg \text{person})),$$

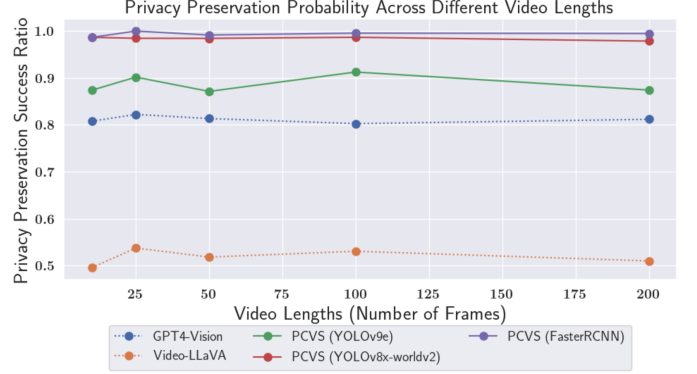


Figure 6: The comparisons between our method and other benchmarks and the comparisons between our method under different object detection models.

which requires hiding all cars, buses, bicycles, and persons appearing in the scenes. Figure 3 (bottom left) demonstrates the successful performance of our method in concealing objects that are irrelevant to the monitoring task, yet require privacy preservation. The demonstration also indicates the real-time capability of our method to be seamlessly migrated to real-world drone applications.

VI. QUANTITATIVE ANALYSES

We present quantitative analyses in two areas: preserving privacy and preserving non-private visual features. We use YOLOv9 [27] on large-scale image datasets—ImageNet [9] and MS COCO [15]—and a real-world driving dataset—UFPR-ALPR [13].

Our analyses show PCVS can preserve privacy even for long-horizon videos with complex privacy specifications. We define the **complexity of specifications**, ϕ , as the *number of propositions* in Φ . For instance, the complexity of a specification $\Phi = \Box(\neg p_1 \wedge \neg p_2 \vee \neg p_3)$ with propositions $AP = \{p_1, p_2, p_3\}$ is $\phi = 3$.

Evaluation Dataset I (ED 1): We focus on the presence of “person” in videos. We select images of a person from the ImageNet dataset and randomly insert these images at various positions for each video duration, filling any remaining slots with random images. We produce five different video lengths: 10, 25, 50, 100, and 200, with 25 video samples for each duration, resulting in 125 video samples overall.

Evaluation Dataset II (ED 2): We use the MS COCO dataset to evaluate our method at different complexities of specifications because it has multiple labels per image. Each level of specification complexity consists of 20 video samples, with an average of 50 frames per sample, resulting in a total of 160 videos. This dataset was developed using the same process as the ED1 dataset, with modifications made to accommodate the complexity of the specifications. For example, if $\phi = 3$, the privacy specification for the dataset is $\Phi = \neg p_1 \wedge \neg p_2 \wedge \neg p_3$, where p_1 , p_2 , and p_3 are the ground truth labels of the selected image. These images are then randomly placed within the dataset, and the remaining slots are filled with random images.

Privacy Preservation Probability Across Different Video Lengths

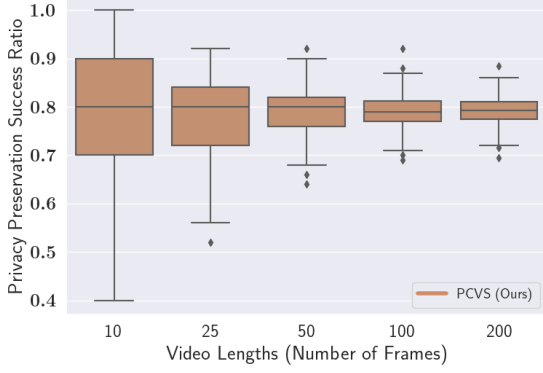


Figure 7: **Effective privacy preservation in real-world driving scenes.** We apply PCVS to driving scenes from the UFPR-ALPR dataset and conceal privacy-sensitive objects such as license plates. The privacy preservation success ratio of PCVS is consistently above 0.8.



Figure 8: Demonstrations on our method concealing license plates in the driving scenes from the UFPR-ALPR dataset.

Evaluation Dataset III (ED 3): We randomly select a subset of images from the UFPR-ALPR dataset [13] to generate videos with lengths 10, 25, 50, 100, and 200. Each length has 200 video samples (a total of 1000 videos). The dataset consists of labeled images that include driving-related objects such as vehicles, license plates, etc. We form a video by integrating a sequence of images from the dataset.

Benchmarks: To assess the ability of PCVS to detect privacy violations based on a given privacy specification, we use GPT-4 Vision [17] and Video LLaVA [14] as benchmarks. This is because both benchmark methods can process a sequence of images from a video alongside a privacy specification.

A. Privacy Preservation

We quantitatively evaluate the performance of privacy preservation across varying video lengths and specification complexities. For this evaluation, we define a metric representing the success ratio of privacy preservation as follows:

$$\text{Privacy Preservation Success Ratio} = \frac{\text{Number of } p_i \in AP \text{ detected or concealed}}{\text{Total number of private } p_i \in AP \text{ within } \mathcal{V}}.$$

Performance on Non-Private Visual Features Preservation

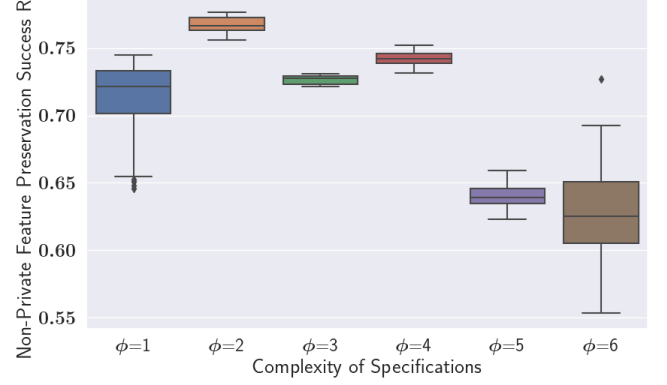


Figure 9: **Preserving non-private visual features for vision-based robot operation.** Our method can detect non-private objects after concealing private objects specified in Φ . However, performance degrades from $\phi = 5$ because more private objects get concealed indirectly masking out other objects.

PCVS counts the number of concealed objects, while the benchmark counts the number of detected objects, as the benchmark does not natively conceal those objects. We assume that if those objects are detected, they can be concealed by other methods such as Gaussian concealing.

a) Comparison by video length: Our method ensures privacy preservation in live video streams, which means that the video length can be infinite. Hence, it is crucial to assess whether privacy is maintained as video streams become longer. To this end, we test PCVS on videos with various lengths from ED 1. We find that PCVS consistently maintains performance in preserving privacy, in contrast to benchmark methods that exhibit degraded performance as the length of videos increases (see Figure 5a).

We also examine how the underlying vision model ability affects the privacy preservation ratio. We repeat the experiment on ED 1 while using different detection models: Yolov9e [27], Yolov8x-worldv2 [5], and FasterRCNN [20], all with default parameters. We present the privacy preservation success ratio of our method using different detection models versus video lengths in Figure 6. The results show that our method is sensitive to the detection model quality. Our method outperforms the benchmarks (GPT4-Vision and Video-LLaVA) at every video length when using the mainstream detection models.

To further demonstrate the real-world applicability of our method, we apply it to ED 3 and evaluate the privacy preservation success ratio across different video lengths. Recall that ED 3 consists of images collected from vehicle dash cameras. Figure 7 shows our method’s high privacy preservation success ratio—consistently above 0.8 regardless of length. We present some demonstration figures in Figure 8. The results indicate the applicability of our method to real-world tasks such as autonomous driving.

b) Comparison by specification complexities: Next, we assess PCVS based on the complexity of specifications. This comparison is important because a privacy specification can be

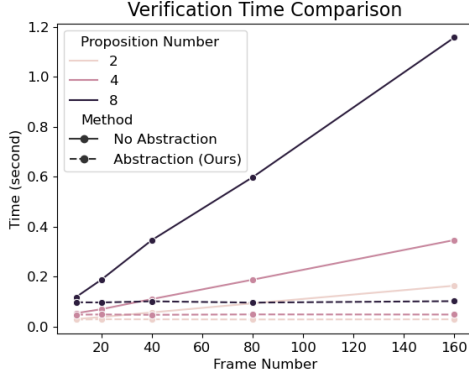


Figure 10: Comparison between the verification time with and without model abstraction. Our model abstraction significantly reduces the latency and remains constant latency when the proposition number increases.

intricate, involving more than just two or three propositions. For example, a specification might require the detection and concealment of multiple privacy-sensitive objects within the same video, such as faces, license plates, and specific types of clothing. Our method significantly outperforms benchmark methods (see Figure 5b) regardless of the complexity of specifications. We demonstrate that PCVS can effectively handle highly complex privacy compositions in real-time video streams, ensuring robust privacy protection.

B. Non-private Visual Feature Preservation

Preserving non-private visual features is crucial for vision-based robot operation, as it relies on visual observation for control policies. In our demonstration (as presented in Figure 3), the ground robot must be capable of identifying people from privacy-constrained video footage to make appropriate decisions, such as stopping. We analyze how our method preserves non-private visual features using ED2 in Figure 9. We define a metric that represents the success ratio of preserving non-private visual features as follows:

$$\text{Non-Private Feature Preservation Success Ratio} = \frac{\text{Number of } \chi \text{ detected after concealing } p_i \in AP}{\text{Total number of } \chi \text{ within } \mathcal{V}},$$

where χ is a non-private target object for detection. In our evaluation, non-private visual features remain preserved and detectable even after the concealment of privacy-sensitive objects as defined in the privacy specifications. However, the success ratio of non-private preservation decreases as the complexity of these specifications increases. This is because PCVS conceals a larger image area as the number of privacy-sensitive objects increases.

C. Computational Complexity

Model checking often incurs significant computational overhead, particularly as the state space size increases with the number of video frames, which limits its capability in real-time applications. Hence, we develop an abstraction method to resolve this limitation.

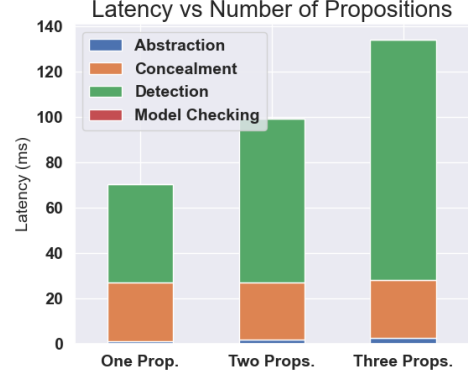


Figure 11: Latency comparison in each stage of our method to process one frame. Object detection takes the major proportion of the time and the time grows linearly as the number of propositions increases. The time for other stages is negligible or remains constant across different numbers of propositions.

Figure 10 shows the verification time versus the frame number under different numbers of atomic propositions. The experiments are performed using the video collected by the ground robot under an *Apple M2 CPU*. As the frame number increases, the verification time without our video abstraction method grows linearly, while the time with abstraction remains constant.

Furthermore, we tested our method with YOLOv9 on both *Intel Xeon gold CPU* and *Nvidia A5000 GPU*. The average runtimes for processing one proposition in one image frame (1600x900 pixels) using CPU and GPU are 159 milliseconds and 69 milliseconds. Therefore, a robot with a CPU can also preserve privacy in real-time at an approximate 6 frames per second (fps) frequency and a robot with a GPU is capable of videos with 14 fps. We present more details in Figure 11.

VII. CONCLUSION

a) *Summary:* We propose PCVS, a method to protect privacy in a live video stream that is either generated from robotic tasks or fed to robot learning algorithms with a probabilistic guarantee of the privacy specification being satisfied. Our method significantly outperforms state-of-the-art methods for short and long video sequences. Further, we show the real-time capabilities of our method on three robotic applications.

b) *Limitations and Future Work:* Our method is limited by the capabilities of the VLM that we use. We are currently unable to process specifications that are action-based in nature (e.g., remove humans who are seen eating in a video) because of the limited performance of the VLM (in the experiment) in action recognition. A future direction is to address this limitation by integrating models that process multiple frames at a time to detect whether an action has occurred. Another future direction is extending our privacy specifications to generic specifications that can describe more properties besides safety, such as liveness and fairness, improving the generalizability of our method.

REFERENCES

- [1] Christel Baier and Joost-Pieter Katoen. *Principles of model checking*. MIT press, 2008.
- [2] Jon Barwise. An introduction to first-order logic. In *Studies in Logic and the Foundations of Mathematics*, volume 90, pages 5–46. Elsevier, 1977.
- [3] Neel P Bhatt, Yunhao Yang, Rohan Siva, Daniel Milan, Ufuk Topcu, and Zhangyang Wang. Know where you’re uncertain when planning with multimodal foundation models: A formal framework. *arXiv preprint arXiv:2411.01639*, 2024.
- [4] Frank Cangialosi, Neil Agarwal, Venkat Arun, Srinivas Narayana, Anand Sarwate, and Ravi Netravali. Privid: practical, {Privacy-Preserving} video analytics queries. In *19th USENIX Symposium on Networked Systems Design and Implementation (NSDI 22)*, pages 209–228, 2022.
- [5] Tianheng Cheng, Lin Song, Yixiao Ge, Wenyu Liu, Xinggang Wang, and Ying Shan. Yolo-world: Real-time open-vocabulary object detection. *arXiv preprint arXiv:*, 2024.
- [6] Yu Cheng, Quanfu Fan, Sharath Pankanti, and Alok Choudhary. Temporal sequence modeling for video event detection. In *Proceedings of the IEEE conference on computer vision and pattern recognition*, pages 2227–2234, 2014.
- [7] Minkyu Choi, Harsh Goel, Mohammad Omama, Yunhao Yang, Sahil Shah, and Sandeep Chinchali. Neuro-symbolic video search. *arXiv preprint arXiv:2403.11021*, 2024.
- [8] Kuan-Yu Chu, Yin-Hsi Kuo, and Winston H Hsu. Real-time privacy-preserving moving object detection in the cloud. In *Proceedings of the 21st ACM international conference on Multimedia*, pages 597–600, 2013.
- [9] Jia Deng, Wei Dong, Richard Socher, Li-Jia Li, Kai Li, and Li Fei-Fei. Imagenet: A large-scale hierarchical image database. In *2009 IEEE conference on computer vision and pattern recognition*, pages 248–255. Ieee, 2009.
- [10] Eileen Guo. A roomba recorded a woman on the toilet. how did screenshots end up on facebook?, Mar 2024.
- [11] Dima Kagan, Galit Fuhrmann Alpert, and Michael Fire. Zooming into video conferencing privacy. *IEEE Transactions on Computational Social Systems*, 2023.
- [12] Hildegard Kuehne, Hueihan Jhuang, Estíbaliz Garrote, Tomaso A. Poggio, and Thomas Serre. HMDB: A large video database for human motion recognition. In Dimitris N. Metaxas, Long Quan, Alberto Sanfeliu, and Luc Van Gool, editors, *IEEE International Conference on Computer Vision*, pages 2556–2563. IEEE Computer Society, 2011.
- [13] R. Laroca, E. Severo, L. A. Zanlorensi, L. S. Oliveira, G. R. Gonçalves, W. R. Schwartz, and D. Menotti. A robust real-time automatic license plate recognition based on the YOLO detector. In *International Joint Conference on Neural Networks (IJCNN)*, pages 1–10, July 2018. doi: 10.1109/IJCNN.2018.8489629.
- [14] Bin Lin, Yang Ye, Bin Zhu, Jiayi Cui, Munan Ning, Peng Jin, and Li Yuan. Video-llava: Learning united visual representation by alignment before projection, 2023.
- [15] Tsung-Yi Lin, Michael Maire, Serge J. Belongie, Lubomir D. Bourdev, Ross B. Girshick, James Hays, Pietro Perona, Deva Ramanan, Piotr Dollár, and C. Lawrence Zitnick. Microsoft COCO: common objects in context. *CoRR*, abs/1405.0312, 2014. URL <http://arxiv.org/abs/1405.0312>.
- [16] Christopher Neff, Matías Mendieta, Shrey Mohan, Mohammadreza Baharani, Samuel Rogers, and Hamed Tabkhi. Revamp 2 t: real-time edge video analytics for multicamera privacy-aware pedestrian tracking. *IEEE Internet of Things Journal*, 7(4):2591–2602, 2019.
- [17] OpenAI. Gpt-4 vision system card. https://cdn.openai.com/papers/GPTV_System_Card.pdf, 2023. Accessed: [insert date of access].
- [18] Arthi Padmanabhan, Neil Agarwal, Anand Iyer, Ganesh Ananthanarayanan, Yuanchao Shu, Nikolaos Karianakis, Guoqing Harry Xu, and Ravi Netravali. Gemel: Model merging for {Memory-Efficient}, {Real-Time} video analytics at the edge. In *20th USENIX Symposium on Networked Systems Design and Implementation (NSDI 23)*, pages 973–994, 2023.
- [19] Sk Md Mizanur Rahman, M Anwar Hossain, Hussein Mouftah, Abdulmotaleb El Saddik, and Eiji Okamoto. Chaos-cryptography based privacy preservation technique for video surveillance. *Multimedia systems*, 18: 145–155, 2012.
- [20] Shaoqing Ren, Kaiming He, Ross Girshick, and Jian Sun. Faster r-cnn: Towards real-time object detection with region proposal networks. *IEEE transactions on pattern analysis and machine intelligence*, 39(6):1137–1149, 2016.
- [21] Nicholas Rescher and Alasdair Urquhart. *Temporal logic*, volume 3. Springer Science & Business Media, 2012.
- [22] Glenn Shafer and Vladimir Vovk. A tutorial on conformal prediction. *Journal of Machine Learning Research*, 9(3), 2008.
- [23] S. P. Sharan, Minkyu Choi, Sahil Shah, Harsh Goel, Mohammad Omama, and Sandeep Chinchali. Neuro-symbolic evaluation of text-to-video models using formal verification, 2024. URL <https://arxiv.org/abs/2411.16718>.
- [24] Nehemia Sugianto, Dian Tjondronegoro, Rosemary Stockdale, and Elizabeth Irenne Yuwono. Privacy-preserving ai-enabled video surveillance for social distancing: Responsible design and deployment for public spaces. *Information Technology & People*, 37(2):998–1022, 2024.
- [25] Elena Umili, Roberto Capobianco, Giuseppe De Giacomo, et al. Grounding ltl specifications in images. In *Proceedings of the 16th International Workshop on Neural-Symbolic Learning and Reasoning*, pages 45–63, 2022.
- [26] Maneesh Upmanyu, Anoop M Namboodiri, Kannan Sri-

nathan, and CV Jawahar. Efficient privacy preserving video surveillance. In *2009 IEEE 12th international conference on computer vision*, pages 1639–1646. IEEE, 2009.

- [27] Chien-Yao Wang, I-Hau Yeh, and Hong-Yuan Mark Liao. Yolov9: Learning what you want to learn using programmable gradient information. In *European Conference on Computer Vision*, pages 1–21. Springer, 2025.
- [28] Junjue Wang, Brandon Amos, Anupam Das, Padmanabhan Pillai, Norman Sadeh, and Mahadev Satyanarayanan. A scalable and privacy-aware iot service for live video analytics. In *Proceedings of the 8th ACM on Multimedia Systems Conference*, pages 38–49, 2017.
- [29] Jehan Wickramasuriya, Mohammed Alhazzazi, Mahesh Datt, Sharad Mehrotra, and Nalini Venkatasubramanian. Privacy-protecting video surveillance. In *Real-Time Imaging IX*, volume 5671, pages 64–75. SPIE, 2005.
- [30] Jim Woodcock, Peter Gorm Larsen, Juan Bicarregui, and John Fitzgerald. Formal methods: Practice and experience. *ACM Comput. Surv.*, 41(4), oct 2009. ISSN 0360-0300. doi: 10.1145/1592434.1592436. URL <https://doi.org/10.1145/1592434.1592436>.
- [31] Yunhao Yang, Jean-Raphaël Gaglione, Sandeep Chinchali, and Ufuk Topcu. Specification-driven video search via foundation models and formal verification. *arXiv preprint arXiv:2309.10171*, 2023.
- [32] Yunhao Yang, Neel P Bhatt, Tyler Ingebrand, William Ward, Steven Carr, Atlas Wang, and Ufuk Topcu. Fine-tuning language models using formal methods feedback: A use case in autonomous systems. *Proceedings of Machine Learning and Systems*, 6:339–350, 2024.
- [33] Meng Yuan, Seyed Yahya Nikouei, Alem Fitwi, Yu Chen, and Yunxi Dong. Minor privacy protection through real-time video processing at the edge. In *2020 29th International Conference on Computer Communications and Networks (ICCCN)*, pages 1–6. IEEE, 2020.